

Strong interactions between free-surface aeration and turbulence down a staircase channel

Hubert CHANSON and Luke TOOMBES

Department of Civil Engineering
 The University of Queensland, Brisbane, 4072 AUSTRALIA

Abstract

Interactions between turbulent waters and the atmosphere may lead to air-water mixing. This experimental study is focused on the flow down a staircase channel characterised by very-strong interfacial aeration and turbulence. Interfacial aeration is characterised by several types of air-water flow structures. The sizes of bubbles and droplets extend over several orders of magnitude, and a significant number of bubble clusters was observed. Velocity and turbulence intensity measurements suggest high levels of turbulence across the entire air-water flow, much higher than in classical monophasic flow situations. Altogether the study provides a new understanding of the basic interfacial processes in aeration cascades.

Introduction

The interactions between flowing waters and the atmosphere may lead to strong air-water mixing and complex multiphase flow situations. Air-water flows have been studied only recently. Although early observations of 'white water' include Leonardo da Vinci, Wen Cheng Ming, and Katsushita Hokusai, the first successful experiments were those of R. Ehrenberger in Austria and later the works led by L.G. Straub in North-America. Since the 1960s, numerous researchers studied gas entrainment in liquid flows. Most studies focused on low void fractions ($C < 5\%$). Few research projects have been engaged in strongly-turbulent flows associated with strong free-surface aeration (Wood 1991, Chanson 1997).

air-water mix consists of water surrounding air bubbles (bubbly flow, $C < 30\%$), air surrounding water droplets (spray, $C > 70\%$) and an intermediate flow structure for $0.3 < C < 0.7$ (Fig. 1). Waves and wavelets may propagate along the free surface.



Fig. 2 – Turbulent flows down a stepped chute. Top : Transition flow ($q_w = 0.108 \text{ m}^2/\text{s}$, $h = 0.1 \text{ m}$, $l = 0.35 \text{ m}$); detail of air-water flow structures with probe in foreground, view from upstream . Bottom : Skimming flow ($q_w = 0.114 \text{ m}^2/\text{s}$, $h = 0.1 \text{ m}$, $l = 0.25 \text{ m}$); flow from the left to the right

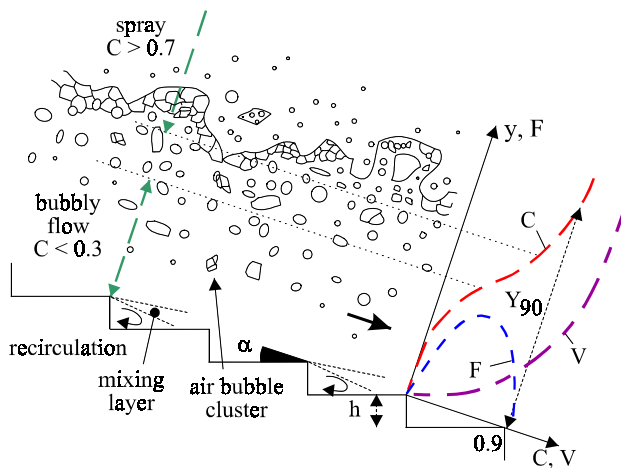


Fig. 1 - Free-surface aeration down a stepped cascade : definition sketch

In open channel flows, free-surface aeration is caused by turbulence fluctuations acting next to the air-water free surface. Through this interface, air is continuously trapped and released. Interfacial aeration involves both entrainment of air bubbles and formation of water droplets. The exact location of the interface becomes undetermined, and there are continuous exchanges of air-water and of momentum between water and atmosphere. The

Highly turbulent flows are experienced down a staircase channel. Low flows behave as a succession of free-falling nappes called nappe flow regime, and little aeration is observed (Rajaratnam 1990, Chanson 1995). With increasing flow rates, a transition flow regime occurs at intermediate discharges. A dominant flow feature is the chaotic appearance with irregular droplet ejections seen to reach heights of up to 3 to 5 times the step height. At larger flow rates, the waters skim over the pseudo-bottom formed by the step edges (skimming flow regime, Fig. 2 Bottom). Intense cavity recirculation is observed and the flow resistance is form drag predominantly. In transition and skimming flows, free-surface aeration is very intense.

It is the aim of this work to describe highly turbulent free-surface flows, and to present new evidence leading to a better understanding of the multiphase flow dynamics. The study examines cascading waters down a stepped chute (Fig. 1 and 2). The structure of the air-water flows is described, and a new analysis of the bubbly flow and spray is presented.

Experimental Apparatus and Instrumentation

Experiments were conducted at the University of Queensland in a 1-m wide stepped chute (Fig. 2). The test section consisted of a broad-crest followed by nine identical steps ($h = 0.1$ m) made of marine ply. Two chute slopes were investigated : $\alpha = 15.9^\circ$ and 21.8° ($l = 0.35$ & 0.25 m respectively). The flow rate was delivered by a pump controlled with an adjustable frequency AC motor drive, enabling an accurate discharge adjustment in a closed-circuit system. The discharge was measured from the upstream head above crest with an accuracy of about 2%. Air-water flow properties were measured using a double-tip probe ($\varnothing = 0.025$ mm). The probe sensors were aligned in the flow direction and excited by an air bubble detector (AS25240). The probe signal was scanned at 20 kHz per sensor for 20 seconds. The translation of the probe in the direction normal to the channel invert was controlled by a fine adjustment travelling mechanism connected to a Mitutoyo™ digimatic scale unit. The error on the vertical position of the probe was less than 0.025 mm. Flow visualisations were conducted with a digital video-camera and high-speed still photographs (e.g. Fig. 2).

Experimental investigations were conducted for flow rates ranging from 0.046 to 0.182 m³/s although the focus was on the highly aerated transition and skimming flows. Measurements were conducted at the outer step edges. Note that uniform equilibrium flow conditions were not achieved at the downstream end of the chute because the flume was relatively short. More details were given in Chanson and Toombes (2001).

Advective Diffusion of Air Bubbles

Downstream of the inception point of free-surface aeration, air and water are fully mixed, forming a homogeneous two-phase flow (Chanson 1997). The advective diffusion of air bubbles may be described by simple analytical models. In transition flows, the distributions of void fraction follow closely :

$$C = K' * \left(1 - \exp\left(-\lambda * \frac{y}{Y_{90}}\right) \right) \quad (1)$$

where y is distance measured normal to the pseudo-invert, Y_{90} is the characteristic distance where $C = 90\%$, K' and λ are dimensionless functions of the mean air content only. Equation (1) compares favourably with experimental data (Fig. 3, Top) but for the first step edge downstream of the inception point of free-surface aeration and for the deflecting jet flow.

In skimming flows, the air concentration profiles may be modelled by :

$$C = 1 - \tanh^2 \left(K' - \frac{y}{2 D_0} + \frac{\left(\frac{y}{Y_{90}} - \frac{1}{3}\right)^3}{3 * D_0} \right) \quad (2)$$

where K' is an integration constant and D_0 is a function of the mean void fraction only. Data are compared successfully with Equation (2) (Fig. 3 Bottom). Although Figure 3 highlights different shapes of void fraction distribution between transition and skimming flows, Equations (1) and (2) are theoretical solutions of the advection diffusion equation for air bubbles assuming different air bubble diffusivity profiles (Chanson and Toombes 2001).

Figure 4 presents dimensionless distributions of bubble count rates $F * d_c / V_c$, where d_c is the critical depth and V_c is the critical flow velocity. The data are compared with parabolic curves. Toombes (2002) demonstrated the unicity of the relationship between bubble frequency and void fraction, and he proposed a sophisticated model comparing favourably with experimental data obtained in water jets discharging into air, smooth-chute flows and stepped chute flows.

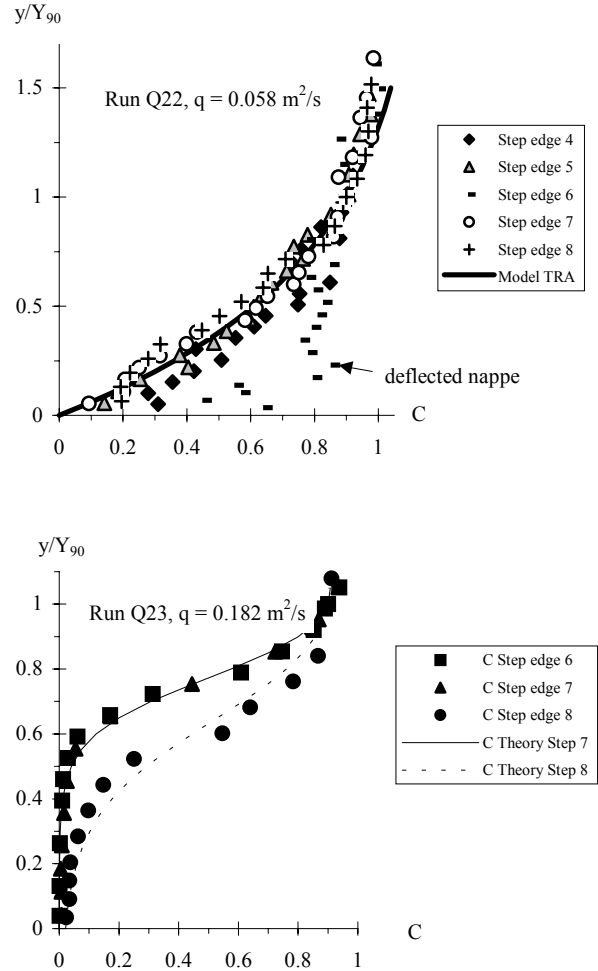


Fig. 3 - Dimensionless distributions of void fraction in stepped chute flow ($\alpha = 21.8^\circ$, $h = 0.1$ m) (data measured at outer step edges). Top : Transition flow, $q_w = 0.058$ m²/s. Bottom: Skimming flow : $q_w = 0.182$ m²/s

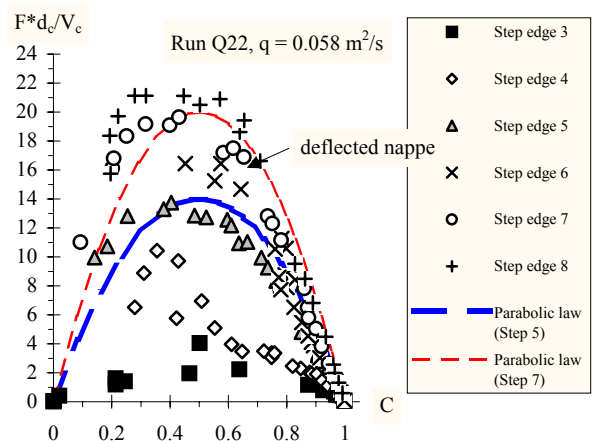


Fig. 4 - Dimensionless bubble count rate distributions ($h = 0.1$ m, $l = 0.35$ m) - Transition flow, $q_w = 0.058$ m²/s

Turbulent Velocity Field

Air-water velocity distributions are presented in Figure 5 in terms of the time-averaged air-water velocity V and turbulence intensity $Tu' = u'/V$. Details of the processing technique were given in Chanson and Toombes (2001). Figure 5 includes transition and skimming flow data for the same flow conditions

as in Figures 3 and 4. In skimming flows, the velocity data compare favourably with a power law (Fig. 5 Bottom). The distributions of turbulence intensity Tu' exhibit relatively uniform profiles implying high turbulence levels across the entire air-water flow mixture (i.e. $0 \leq y \leq Y_{90}$) (Fig. 5). The trend, observed in both skimming and transition flows, differs significantly from well-known turbulence intensity profiles observed in turbulent boundary layers (e.g. Schlichting 1979). It is believed that the high rate of energy dissipation, associated with form drag generated by the steps, contributes to strong turbulent mixing throughout the entire flow. Although the quantitative values of turbulence intensity are large ($\sim 100\%$), they are similar to turbulence measurements in separated flows past rectangular cavity (Haugen and Dhanak 1966), in wakes between large stones (Sumer et al. 2001) and in developing shear region of plunging water jets (Chanson and Brattberg 1998).

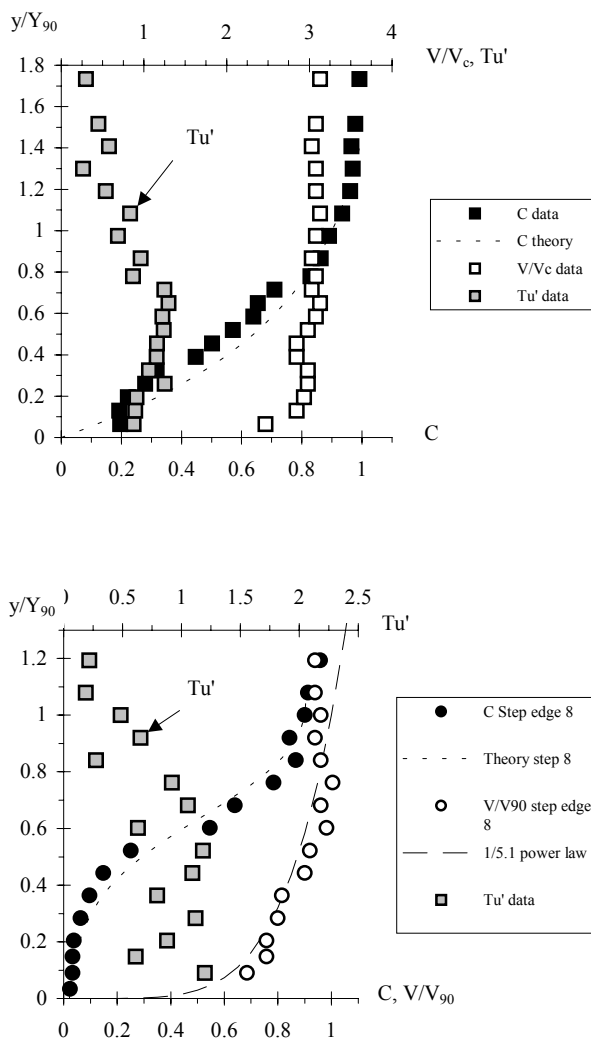


Fig. 5 - Dimensionless velocity and turbulent intensity distributions (measured at the last step edge, $\alpha = 21.8^\circ$). Top : Transition flow : $q_w = 0.058 \text{ m}^2/\text{s}$, $V_c = 0.83 \text{ m/s}$. Bottom : Skimming flow : $q_w = 0.182 \text{ m}^2/\text{s}$, $V_{90} = 3.47 \text{ m/s}$

Characteristic Bubble/Droplet Sizes

Figure 6 presents normalised probability distribution functions of bubble and droplet sizes. Each histogram column represents the probability of bubble/droplet chord length in 0.5 mm intervals : e.g., the probability of chord length from 3.0 to 3.5 mm is represented by the column labelled 3.0. The last column indicates the probability of chord lengths larger than 20 mm.

The results show a broad spectrum of bubble and droplet chord lengths at each location. The chord length distributions are typically skewed with a preponderance of small bubble/droplet sizes relative to the mean. The probability of air bubble chord lengths is the largest for bubble sizes between 0 and 2.5 mm for $C \leq 0.2$ (Fig. 6 Top). It is worth noting the amount of bubbles larger than 20 mm. Although water droplet chord distributions appear skewed with a preponderance of small droplet sizes relative to the mean, the distributions differ from bubble chord length distributions. For the same void and liquid fraction, the droplet chord mode and mean are larger than the corresponding bubble chord length data (Fig. 6).

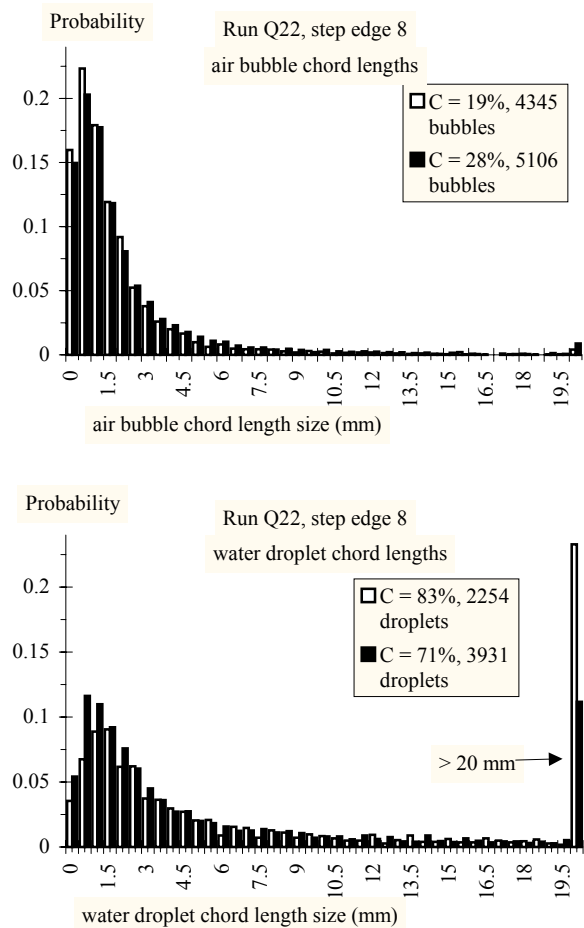


Fig. 6 - Bubble and droplet chord length distributions in transition flow ($q_w = 0.058 \text{ m}^2/\text{s}$, $\alpha = 21.8^\circ$). Top : air bubble chord lengths. Bottom : droplet chord lengths

Bubble and Droplet Clusters

The spatial distribution of bubbles and droplets was analysed. In bubbly flow (i.e. $C < 0.3$), two bubbles were considered to form a cluster when they were separated by a water chord length smaller than 1 mm. Such a distance is about 20 to 50 times smaller than the mean water chord length in the bubbly flow region ($C < 0.3$). It is about the bubble size for which the coalescence probability of larger bubbles is negligible (Chesters

1991, p. 268) and the length scale for bubble breakup in shear flows (Chanson 1997, p. 229) assuming a 0.5 m/s velocity.

In skimming flows, 27% of air bubbles in average were associated with bubble clusters, almost independently of void fractions and mean chord length sizes. The average size of cluster bubbles was about 14% larger than the average bubble size. Nearly 76% of clusters comprised of two bubbles (Fig. 7). In transition flows, 37% of the bubbles in average were grouped in clusters, while about 74% of the clusters were made of two bubbles.

A similar analysis of droplet clusters was performed in the spray region (i.e. $C > 0.7$). Two droplets were assumed to form a platoon if they were separated by an air chord length smaller than 1 mm. In skimming flows, the results showed a small number of droplet clusters: i.e., an average 11% of detected droplets formed a cluster, and about 89% of clusters included two droplets only. In transition flows, an average 19% of droplets were parts of clusters, and in average 83% of clusters comprised two droplets only. For the same void and liquid fraction, the probability of a bubble to travel as part of a cluster was larger than the probability of a droplet to travel in a platoon.

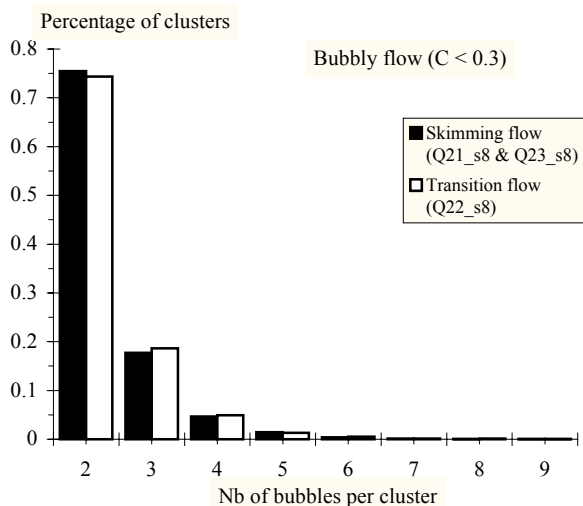


Fig. 7 - Number of bubbles per cluster in bubbly flows ($C < 0.3$, $\alpha = 21.8\%$). Skimming flow: 17,834 detected bubbles, 2,796 bubble clusters. Transition flow: 37,454 bubbles, 4,580 clusters.

Discussion

A sensitivity analysis was performed in bubbly flows ($C < 0.3$, skimming flows) to ascertain the representativity of the results. It was shown that the number of detected bubbles N_{ab} had to be greater than 800 to 900 for the cluster analysis results to be within 10% of the mean value, in terms of number of clusters, number of bubbles per cluster and size of bubbles in clusters. Further the cluster analysis highlighted the dual requirements to record a large number of bubble/droplet detections to improve the representativity of the samples, and to detect small water/air chord lengths associated with thin bubble/droplet interfaces. The writers believe that the present data acquisition rate (20 kHz per sensor for 20 s) was adequate in bubbly flows, but longer recording times are required in the spray region.

Summary and Conclusions

Detailed air-water flow measurements were conducted down a stepped cascade. The study demonstrates the strong aeration (Fig. 2, 3 & 4) generated by high turbulence levels extending from the stepped invert up to the pseudo free-surface (Fig. 5).

Air bubble and water droplet measurements highlight the broad spectrum of detected bubble/droplet sizes extending from less than 0.2 mm to over 20 mm (Fig. 6). In the bubbly flow region ($C < 0.3$), about 25% of detected bubbles were parts of bubble clusters. Most clusters comprised of two bubbles with no obvious preferential sizes (Fig. 7).

Overall the large numbers of entrained bubbles/droplets generate large interfacial areas which in turn contribute to substantial air-water mass transfer of atmospheric gases. The results explain the re-oxygenation potential of stepped cascades, used for in-stream re-aeration and in treatment plants.

Acknowledgments

The first writer acknowledges the helpful comments of Dr J.L. Marié (ECL, France).

References

- Chanson, H. (1995). *Hydraulic Design of Stepped Cascades, Channels, Weirs and Spillways*. Pergamon, Oxford, UK
- Chanson, H. (1997). *Air Bubble Entrainment in Free-Surface Turbulent Shear Flows*. Academic Press, London, UK.
- Chanson, H., and Brattberg, T. (1998). "Air Entrainment by Two-Dimensional Plunging Jets: the Impingement Region and the Very-Near Flow Field." *Proc. 1998 ASME Fluids Eng. Conf., FEDSM'98*, Washington DC, USA, Paper FEDSM98-4806, 8 pages (CD-ROM).
- Chanson, H., and Toombes, L. (2001). "Experimental Investigations of Air Entrainment in Transition and Skimming Flows down a Stepped Chute. Application to Embankment Overflow Stepped Spillways." *Research Report No. CE158*, Dept. of Civil Engrg, University of Queensland, Brisbane, Australia
- Chesters, A.K. (1991). "The Modelling of Coalescence Processes in Fluid-Liquid Dispersions: a Review of Current Understanding." *Trans. IChemE*, Vol. 69, Part A, pp. 259-270.
- Haugen, H.L., and Dhanak, A.M. (1966). "Momentum Transfer in Turbulent Separated Flow past a Rectangular Cavity." *Jl of Applied Mech.*, Trans. ASME, Sept., pp. 641-664.
- Rajaratnam, N. (1990). "Skimming Flow in Stepped Spillways." *Jl of Hyd. Engrg.*, ASCE, Vol. 116, No. 4, pp. 587-591.
- Sumer, B.M., Cokgor, S., and Fredsoe, J. (2001). "Suction Removal of Sediment from between Armor Blocks." *Jl of Hyd. Engrg.*, ASCE, Vo. 127, No. 4, pp. 293-306.
- Toombes, L. (2002). "Experimental Study of Air-Water Flow Properties on low-gradient Stepped Cascades." *Ph.D. thesis*, Dept of Civil Engineering, University of Queensland, Brisbane, Australia.
- Wood, I.R. (1991). "Air Entrainment in Free-Surface Flows." *IAHR Hydraulic Structures Design Manual No. 4*, Hydraulic Design Considerations, Balkema Publ., Rotterdam, The Netherlands.